NIH Public Access
Author Manuscript
Dev Biol. Author manuscript; available in PMC 2009 April 1.

Published in final edited form as:
Dev Biol. 2008 April 1; 316(1): 160–170.

The homodimeric kinesin, Kif17, is essential for vertebrate photoreceptor sensory outer segment development

Christine Insinna[*,1], **Narendra Pathak**[*,2], **Brian Perkins**[3], **Iain Drummond**[2], and **Joseph C. Besharse**[**,1]

1*Department of Cell Biology, Neurobiology and Anatomy, Medical College of Wisconsin, 8701 Watertown Plank Rd, Milwaukee, WI 53226, USA*

2*Nephrology Division, Massachusetts General Hospital and Department of Medicine, Harvard Medical School, 149 13th Street, Charlestown, MA 02129*

3*Department of Biology, College of Science, 3258 TAMU, College Station, TX 77843*

Abstract

Sensory cilia and intraflagellar transport (IFT), a pathway essential for ciliogenesis, play important roles in embryonic development and cell differentiation. In vertebrate photoreceptors IFT is required for the early development of ciliated sensory outer segments (OS), an elaborate organelle that sequesters the many proteins comprising the phototransduction machinery. As in other cilia and flagella, heterotrimeric members of the kinesin 2 family have been implicated as the anterograde IFT motor in OS. However, in *C. elegans*, OSM-3, a homodimeric kinesin 2 motor, plays an essential role in some, but not all sensory cilia. Kif17, a vertebrate OSM-3 homologue, is known for its role in dendritic trafficking in neurons, but a function in ciliogenesis has not been determined. We show that in zebrafish Kif17 is widely expressed in the nervous system and retina. In photoreceptors Kif17 co-localizes with IFT proteins within the OS, and co-immunoprecipitates with IFT proteins. Knockdown of Kif17 has little if any effect in early embryogenesis, including the formation of motile sensory cilia in the pronephros. However, OS formation and targeting of the visual pigment protein is severely disrupted. Our analysis shows that Kif17 is essential for photoreceptor OS development, and suggests that Kif17 plays a cell type specific role in vertebrate ciliogenesis.

Keywords

Kif17; photoreceptors; cilia; ciliogenesis; IFT; zebrafish

Introduction

Ciliogenesis is of great current interest in developmental biology because components of important signaling pathways such as hedgehog (Corbit et al., 2005), and PDGFα (Schneider et al., 2005) are sequestered within cilia and require both developmental and constitutive ciliogenesis pathways for their function (Caspary et al., 2007; Eggenschwiler and Anderson, 2007). For example, during sonic hedgehog (Shh) signaling the patched receptor (Ptc) in the

**Correspondence: Dr. Joseph C. Besharse, Department of Cell Biology, Neurobiology and Anatomy, Medical College of Wisconsin, 8701 Watertown Plank Rd, Milwaukee, WI 53226, Telephone: (414) 456-8260, Fax: (414) 456-6517, Email: jbeshars@mcw.edu.
*These two authors contributed equally to the work.

Publisher's Disclaimer: This is a PDF file of an unedited manuscript that has been accepted for publication. As a service to our customers we are providing this early version of the manuscript. The manuscript will undergo copyediting, typesetting, and review of the resulting proof before it is published in its final citable form. Please note that during the production process errors may be discovered which could affect the content, and all legal disclaimers that apply to the journal pertain.

NIH-PA Author Manuscript
NIH-PA Author Manuscript
NIH-PA Author Manuscript

NIH-PA Author Manuscript

NIH-PA Author Manuscript

NIH-PA Author Manuscript

cilium membrane, on binding by Shh, translocates to the cell body at the same time that smoothened (Smo) moves into the cilium membrane (Rohatgi et al., 2007). Thus, the fundamental pathway for ciliogenesis regulates the initial location of Ptc, as well as the subsequent translocation of Smo, and processing of Gli transcription factors.

Ciliogenesis in motile cilia and flagella as well as in sensory cilia requires a pathway called intraflagellar transport (IFT). IFT involves the bidirectional movement of multi-protein IFT particles along the microtubules of ciliary axonemes (Rosenbaum and Witman, 2002). IFT functions to transport molecular cargo, including components of the axoneme itself and membrane proteins (Hou et al., 2007; Qin et al., 2005) as well as key elements involved in intracellular signaling (Pan et al., 2005). Both the IFT complex proteins and molecular motors of IFT are highly conserved among all types of eukaryote cilia including sensory cilia. Of particular relevance is the finding that heterotrimeric kinesin 2 family members, referred to here as the Kif3 complex, are required for anterograde IFT (Rosenbaum and Witman, 2002).

Although the Kif3 complex is associated with IFT in every system studied to date, recent work in *C. elegans* has implicated other kinesin motors in sensory cilium trafficking (Evans et al., 2006; Pan et al., 2006; Peden and Barr, 2005; Snow et al., 2004). In particular, OSM-3, a homodimeric member of the kinesin 2 family, serves as an accessory IFT motor in amphid channel sensory cilia. In these cilia, OSM-3 is required for elongation of singlet microtubules in the distal segment of the cilium (Evans et al., 2006; Snow et al., 2004). Furthermore, in AWB cilia OSM-3 can act independently of the Kif3 complex (Mukhopadhyay et al., 2007). Understanding which motors are critical in ciliogenesis in vertebrates is clearly important, but at present the question of whether additional kinesin motors play a role in organisms other than *C. elegans* remains un-resolved.

Both the Kif3 complex (Jimeno et al., 2006; Marszalek et al., 2000) and IFT proteins (Pazour et al., 2002; Baker et al., 2003) are necessary for photoreceptor OS assembly in vertebrates. However, electron microscopy has shown that vertebrate photoreceptors (Roof et al., 1991; Steinberg and Wood, 1975), like amphid channel cilia in *C. elegans* (Evans et al., 2006), have distal singlet extensions of their axoneme. The requirement of OSM-3 kinesin for distal elongation specifically in cilia with singlet extensions led us to test the idea that photoreceptor OS assembly would require Kif17, an OSM-3 homologue. We show here that Kif17 is closely associated with the photoreceptor OS axoneme and both co-localizes and co-immunoprecipitates with IFT proteins. Furthermore zebrafish deficient in Kif17 during early development have severely disrupted OS development with mis-targeting of their visual pigment. In contrast, kidney epithelial cilia elongate normally. These results indicate that Kif17 is required for photoreceptor OS formation and protein targeting and indicate that the role of Kif17 differs among different sensory cilium types in vertebrates.

Materials and methods

Antibodies

A polyclonal anti-Kif17 antibody and monoclonal anti-cyclic nucleotide gated channel 1 (CNG1) and anti-acetylated-α-tubulin antibodies were obtained from Abcam, Cambridge, MA and Sigma-Aldrich, St. Louis, MO respectively. The rabbit anti-IFT57 antibody was a gift from Dr. G. Pazour at the University of Massachusetts. The new affinity purified goat anti-mouse IFT52 and guinea pig anti-mouse IFT20 were directed at peptide CLQEGDENPRDFTTLF or full-length recombinant protein respectively; both were custom produced at Covance, Inc. (Madison, WI). The goat anti-IFT88 antibody was described previously (Baker et al., 2003). Zebrafish anti-rhodopsin and anti-cone green ospin antibodies were gifts from Dr T. S. Vihtelic at the University of Notre Dame (Vihtelic et al., 1999). Affinity purified rabbit anti-peptide antibodies directed at zebrafish IFT20 (CEAEQSEFIDQFILQK), IFT57

NIH-PA Author Manuscript

NIH-PA Author Manuscript

NIH-PA Author Manuscript

(CMHATHLLEPNAQAY), and IFT88 (LEFADGELGDDLLPE) were custom produced at Bethyl Laboratories (Montgomery, TX); zebrafish anti-IFT52 was similarly designed and affinity purified at Open Biosystems, Huntsville, AL.

Immunocytochemistry

Three day old control and morphant embryos were fixed 1 hr at room temperature in 4% paraformaldehyde in phosphate buffered saline (PBS; pH 7). After three washes in PBS, embryos were cryprotected in 15% sucrose for 1 hour at 4ºC and then 30% sucrose for 1 hour at 4ºC, embedded in OCT medium (Miles Scientific, Elkhart, IN) and frozen. 10–15 μm sections of retinas were cut on a cryostat, collected on slides, and allowed to air dry for 2 hours at room temperature. Slides were blocked in PBS containing 0.25% TX-100, 5% normal goat serum and 1% BSA for 1 hour at room temperature and incubated in primary antibody overnight at 4ºC or 1 hour at room temperature in a humidified chamber. After three washes in PBS, slides were incubated in secondary antibody (Alexa 488 or 568, Molecular Probes) for 1 hour at room temperature in the dark. Nuclei were stained with Topro-3 (Molecular Probes, Eugene, OR) before the final washes. Sections were mounted in Fluoromount G (Electron Microscopy Sciences, Hatfield, PA) and imaged using a Zeiss LSM410 Confocal Laser Scanning inverted microscope.

For isolated OSs with attached inner segments, fresh wild type retinas from adult zebrafish were collected, shaken gently, and fixed on glass slides with 1% PFA in PHEM (60 mM PIPES, pH 6.9, 25 mM HEPES, 10 mM EGTA and 2 mM $MgCl_2$) overnight at 4ºC. Cells were permeabilized in 0.1% TX-100 in PHEM for 1 hour at room temperature and blocked in 1% BSA in PHEM for 30 minutes at room temperature. Samples were co-stained with antibodies to Kif17 and acetylated-α-tubulin or anti-IFT antibodies as described above. Images were taken using a 100X objective (NA 1.4) on a Bio-Rad MRC 600 confocal microscope.

Immunoprecipitations and western blot

Immunoprecipitations were performed as described previously (Baker et al., 2003) using 14 adult zebrafish retinas dissected after a 1 hour dark adaptation. For western blots, samples were loaded on a 10 % Tris-HCl gel (Biorad, Hercules, CA). Proteins were transferred to an Immobilon transfer membrane (Millipore, Bedford, MA), incubated with primary antibody followed by secondary IgG conjugated to horseradish peroxidase, and visualized with ECL Western Blotting Detection Reagents (GE Healthcare, Buckinghamshire, UK).

Cloning zebrafish *kif17*

The zebrafish *kif17* gene was predicted in genomic sequence (Sanger Center, UK) based on protein homology to the human KIF17 (AAH65927.1) using tblastn. Nested PCR primers to the 5′ and 3′ UTR sequence of the predicted *kif17* cDNA (listed below) were used in RT-PCR performed on total RNA from 2.5 day old zebrafish larvae.

ZKF17F1	GATGGCATCAGAGTCCGTGAAGG
ZKF17F2	CCGTGAAGGTGGTCGTCAGATGT
ZKF17R1	AAAACAGGTCAAGCTCTGGGCTA
ZKF17R2	TTGCGTTTTACTTTGCCGTGTGA

A 2.3 kb *kif17* cDNA was cloned in pCRII-Topo vector (Invitrogen) and sequenced. The Genbank accession number for zebrafish *kif17* is EF507508.

In situ hybridization

Whole mount in situ hybridization was performed as previously described (Thisse et al., 1993). The DIG labeled antisense RNA probe was synthesized by in vitro transcription reaction

NIH-PA Author Manuscript

NIH-PA Author Manuscript

NIH-PA Author Manuscript

using SP6 polymerase (Ambion) and XhoI linearized *kif17*-TopoII clone as template. The stained embryos were dehydrated, cleared with Benzyl benzoate: Benzyl alcohol mix and photographed with a digital Spot camera mounted on a Leica MZ12 stereomicroscope.

Morpholino injection

Antisense morpholino oligonucleotides used to knock-down zebrafish kif17 were ordered from Gene Tools (Corvallis, OR, USA). Sequences of the kif17m and control morpholinos were:

kif17MOex2d:	5′-TTGTAAACTGGTTACCTGGATTGTC-3′
control:	5′-CTGTTAGGTCCATTGGTCAAATGTT-3′.

Morpholinos were injected using a nanoliter 2000 microinjector (World Precision Instruments, Inc) in 1–2 cell stage wild type TuAB embryos, at a concentration of 0.3 mM and injection volume 4.6 nl/embryo. Injected embryos were kept in fish water containing 0.003% 1-phenyl-2-thiourea (PTU) to inhibit development of pigmentation and anesthetized at 3 days post fertilization (dpf). Imaging was performed using a Nikon inverted microscope. Nested RT-PCR was performed to verify the morpholino induced a molecular defect.

Electron microscopy

Three day old control and morphant embryos were prepared for conventional EM in the Medical College of Wisconsin core Electron Microscopy Facility as described previously (Pazour et al., 2002). Sections were observed using a Hitachi 600 electron microscope. Negative images from the EM were digitally scanned at 600 dpi using an Epson 3200 Scanner, and digital images were assembled using Adobe Photoshop.

High speed videomicroscopy

PTU treated embryos (54 hpf) were put in E3 egg water containing 40 mM BDM (2,3-butanedione monoxime, Sigma) for 5 min to stop the heart beat and then changed to 20 mM BDM containing egg water for observation. The embryos were analyzed using a Zeiss Axioplan microscope (Zeiss, Germany) equipped with a high-speed Photron FastCAM-PCI500 video camera (Photron LTD). Images of beating cilia were acquired at 250 frames per second using Photron FastCAM version 1.2.0.7 (Photron LTD). Image processing was done using Adobe Photoshop and movies were compiled in Graphic converter 4.5.2 (Lemke Software, Germany) and Quicktime (Apple, Inc.).

Results

Kif17 is expressed in vertebrate photoreceptors

We initially examined the expression of Kif17 in zebrafish using in situ hybridization (ISH) and immunocytochemistry (IC). Prior studies of Kif17 in mice have established its function in neurons, and consistent with this ISH shows that Kif17 mRNA is highly expressed in the developing nervous system and eye (Figure 1A and C); it is also expressed in the pronephros, olfactory placodes, pectoral fin, and lateral line organs (Figure 1B–D). To evaluate the distribution of Kif17 protein in retina and photoreceptors, we used an antibody that recognizes a single specific protein band in western blots at ~100 kDa in zebrafish embryos (Figure 2A). IC on frozen sections (data not shown) revealed that Kif17 is expressed in all retinal layers, including the photoreceptor layer and retinal pigment epithelium. To study Kif17 at higher resolution, we isolated photoreceptors. Zebrafish have rods, short and long single cones, and short and long double cones, which typically break away from the retina at the narrow myoid region (Figure 2B). In single label experiments, Kif17 was specifically associated with the ciliary axoneme of rods, single cones, and double cones; double-label IC with an antibody to

NIH-PA Author Manuscript

NIH-PA Author Manuscript

NIH-PA Author Manuscript

acetylated α-tubulin (Figure 2C, lower panel) verified that the labeling was axoneme associated. Interestingly, we also noticed that Kif17 fluorescence was higher in cones than in rods (data not shown).

Zebrafish OS axonemes extend microtubule singlets

In all photoreceptor types, Kif17 was found along the entire length of the axoneme (Figure 2C). However, the labeling for both acetylated α-tubulin and Kif17 lost its intensity toward the OS distal end. This is consistent with previous reports that doublet microtubules in photoreceptors loose the B-subfiber and extend distally as singlets (Roof et al., 1991; Steinberg and Wood, 1975); in frogs this transition occurs in the proximal OS (Roof et al., 1991).

To verify the existence of microtubule singlets in the proximal region of zebrafish OS, cross-sections of the axonemal shaft were examined at the EM level (Figure 2D); this examination was restricted to the proximal OS. At the junction of inner and outer segments, the connecting cilium (transition zone) exhibits a typical pattern of 9 doublets (Figure 2D, left). Nine doublets are also seen in the most proximal OS but they are disordered and lie in a cytoplasmic shaft adjacent to the OS discs (Figure 2D, middle). More distally, but still within the proximal one third of the OS, some doublets convert to singlets (Figure 2D). Singlets are routinely detected in the distal outer segment and these data show that singlets are first encountered within the proximal OS.

Kif17 associates with IFT complex proteins in zebrafish photoreceptors

Using antibodies to both mammalian and zebrafish IFT proteins we have found that Kif17 co-localizes and co-immunoprecipitates with IFT proteins. As shown for IFT88 in consecutive confocal Z-sections (Figure 3A), Kif17 co-localizes in punctuate structures with IFT88 in the myoid region (small arrow), at the basal body (BB), and along the axoneme; similar co-localization of Kif17 with IFT52, and IFT20 was also observed (data not shown). Furthermore, we used immunoprecipitation to confirm the association of Kif17 with IFT proteins observed with immunocytochemistry. Antibodies to IFT20, IFT57, IFT88, and Kif17 all IP Kif17 (Figure 3B). Furthermore, anti-IFT57 and Kif17 antibodies precipitated Kif17 as part of a larger complex as demonstrated in reciprocal IP using anti-IFT57 and anti-Kif17 (Figure 3C). Although differences in IP efficiency were detected for different anti-IFT antibodies, those directed at both mouse and zebrafish proteins were effective in bringing down zebrafish retinal Kif17. Since IFT proteins like IFT57 exist almost exclusively in a complex with other IFT proteins (Pazour et al., 2002; Baker et al., 2003), these data imply that Kif17 is part of a larger complex.

Knockdown of Kif17 disrupts photoreceptor cilium and OS formation

In order to evaluate the effects of Kif17 deficiency on zebrafish development, embryos were injected with an antisense morpholino oligonucleotide directed at the Exon 2 splice donor site (Figure 4A). This morpholino was predicted to activate a cryptic splice site in exon 2 and to introduce a premature stop codon. RT-PCR (Figure 4A) showed extreme reduction in the expected WT Kif17 PCR product in embryos at 56 hrs post-fertilization and the appearance of a smaller PCR band. The presence of the expected stop codon in the lower band was confirmed by DNA sequencing (Figure 4B). Furthermore, western blotting of lysate from 3 day old morphants showed that Kif17 protein was dramatically reduced compared to embryos injected with the control sequence (Figure 4D). The Kif17 antibody used in the western blotting was directed at the C-terminal of the protein and as expected, we did not detect a truncated protein.

Overall the morpholino had little effect on early embryogenesis. Three day old morphants were grossly normal and slightly smaller than controls, with occasional slight curvature of the tail (Figure 4C). Recent analysis has indicated that Kif17 is not required for elongation of

NIH-PA Author Manuscript

NIH-PA Author Manuscript

NIH-PA Author Manuscript

mammalian kidney epithelial cilia in culture even though it is implicated in ciliary membrane protein trafficking (Jenkins et al., 2006). Consistent with this, cystic kidneys did not develop and pronephric kidney epithelial cilia were of normal length in 2.5 day old larvae (Table 1). Kidney epithelial cilia are normally motile in zebrafish and differences between control and morpholino injected embryos were not detected in time-lapse analysis of their motility (see Table 1; Quicktime videos included as Supplemental Material).

The principal phenotype in 3 day old morphants was a failure of photoreceptor OS development (Figure 5). First, overall retinal development and lamination to form the outer nuclear (ONL), inner nuclear (INL) and ganglion cell (G) layers occurred in both control and morphant embryos (Figure 5A and C); only in the most severe cases resulting from injection of the highest concentration of morpholino was a small degree of retinal disorganization detected. Control embryos (Figure 5A, B) elongated normal OS with lamellar discs in the space between IS and retinal pigment epithelium (RPE). Morphants, however, exhibited a striking failure of OS formation visible even by light microscopy. In control larvae OS stain darkly (Figure 5A), but in morphants very little OS staining was detected (Figure 5C). EM analysis revealed formation of well ordered OS throughout the retina in controls (Figure 5B) compared to a near total failure of OS formation in the central retina of morphants (Figure 5D). However, in the retinal periphery of morphants, short OS and sensory cilia with aberrant discs were often seen (Figure 5E, F). The latter finding is likely attributable to a decreased effect of the morpholino in the late developing peripheral photoreceptors. An important feature of retinal development is that after initial lamination and differentiation, the retina continues to grow by addition of new photoreceptor cells at the retinal margin. Therefore, the oldest post-mitotic cells are at the retinal center and those at the periphery are derived from precursors that had continued to divide. Since the morpholino was introduced at the one cell stage and is diluted through successive cell divisions over time, differences in the extent of Kif17 knockdown between the central and peripheral retina would be expected. Although the blockade of OS formation in the central retina was often complete at 3 dpf, degenerating photoreceptors were not generally observed and the severity of the OS phenotype was diminished by 4 dpf, an effect attributable to loss of the morpholino effect over time.

To determine if regional differences in OS development were correlated with differences in Kif17 expression, immunocytochemistry (IC) was conducted to monitor the extent of Kif17 knockdown in the eye (Figure 6). In controls, Kif17 was expressed at a high level in photoreceptors and to a lesser extent throughout the retina (Figure 6A and D). In morphants Kif17 staining was reduced overall compared to WT and was virtually undetectable in the photoreceptor layer of the central retina (see asterisks in Figure 6B and E, C and F). Although reduced in level at the retinal margin, the staining pattern in this region was similar to retinas from embryos receiving the control morpholino (see arrows in Figure 6B and E, C and F). In general, the spatial pattern of photoreceptor OS loss matched the spatial pattern of Kif17 knock-down.

Kif17 is required for the trafficking of OS membrane proteins

Finally, we looked at the localization of membrane proteins in rods and cones of control versus morphants using IC. We focused on rod and cone opsins and the rod cyclic nucleotide gated channel (CNG1), because rhodopsin is mis-localized in $Tg737^{orpk}$ mice deficient in IFT88 (Pazour et al., 2002) and because Kif17 has been implicated in ciliary trafficking of the olfactory CNG channel (Jenkins et al., 2006). A lack of characterized CNG antibodies that cross-react with zebrafish cones limited our analysis to CNG1 of rod cells. In rods of controls CNG1 and rhodopsin co-localized and were highly concentrated in the OS, but were undetectable in the rod synaptic terminals of the outer plexiform layer (arrows in Figure 7A, upper panel). In contrast a moderate degree of mis-targeting of both membrane proteins to the

NIH-PA Author Manuscript

NIH-PA Author Manuscript

NIH-PA Author Manuscript

outer plexiform was routinely seen in morphant rods (Figure 7A, lower panel). However, the most striking finding was an extreme degree of cone opsin mis-targeting (Figure 7B). In controls, cone opsin is present exclusively in OS, but in morphants was distributed throughout the plasma membrane of the cone cell body and perinuclear region and accumulated extensively in the synaptic terminals of the outer plexiform layer (Figure 7B); mis-localization of opsin was seen even in cones with partially developed OS. It is likely that the less severe mis-localization of membrane proteins in rods reflects the fact that in 3 day larvae rods are found at retinal periphery where Kif17 knockdown is not complete (see Figure 6). Most of the photoreceptors in the retinal center are cones.

Discussion

Kif17 has been studied previously in the context of dendritic transport in neurons where it was implicated in trafficking of glutamate receptors to the synapse (Guillaud et al., 2003; Kayadjanian et al., 2007; Setou et al., 2000). Our new morpholino knockdown experiments demonstrate that Kif17 is also required for assembly of the photoreceptor sensory OS. Furthermore, the co-localization and co-immunoprecipitation of Kif17 with IFT proteins implies that it functions in photoreceptors within the IFT pathway. In contrast to its essential role in photoreceptors, we also show that Kif17 is not required for elongation or normal motility of cilia in the developing zebrafish pronephros. Our findings in kidney are consistent with the lack of an effect of a dominant negative Kif17 on cilium elongation in cultured kidney epithelial cells (Jenkins et al., 2006). However, in those studies the dominant negative protein did block ciliary targeting of an olfactory cyclic nucleotide gated channel (CNGB1) that had been transfected into the cells (Jenkins et al., 2006), implicating Kif17 in ciliary membrane protein trafficking. In contrast to Kif17, the heterotrimeric Kif3 complex is essential for cilium elongation in kidney epithelial cells (Lin et al., 2003) and in photoreceptor OS formation in mice (Jimeno et al., 2006; Marszalek et al., 2000), suggesting that the Kif3 complex and Kif17 play different roles in photoreceptor and kidney epithelial ciliogenesis. This difference may at least in part reflect differences in the structure of their axonemes.

The analysis of IFT motors in *C. elegans* has led to a model in which the Kif17 homologue, OSM-3, is an accessory IFT motor that functions cooperatively with the Kif3 complex in cilia containing only doublet microtubules, and is essential for elongation of distal singlet extentions in amphid channel cilia (Evans et al., 2006; Pan et al., 2006; Peden and Barr, 2005; Snow et al., 2004). Although axonemes of many ciliary types in vertebrates consist predominantly of doublet microtubules, distal singlet extensions are present in photoreceptors (Roof et al., 1991; Steinberg and Wood, 1975). Furthermore, EM analysis of frog photoreceptors has shown that singlets are present through most of the length of the OS (Roof et al., 1991). Our data indicate that zebrafish photoreceptors are similar to those of frog in that singlets appear within the proximal OS. Although short singlet extensions have been reported in some kidney epithelial cells (Webber and Lee, 1975), the failure to form short singlet extensions in cilia dominated by doublets would likely go un-noticed in our analysis. Thus, the differences between photoreceptors and kidney epithelial cells are consistent with the *C. elegans* model, and suggest that Kif17 could be important for singlet extension in the distal OS.

In morphant retinae differences in the severity of the phenotype were seen between the retinal center and the retinal periphery that correlate with the severity of Kif17 protein knockdown. The phenotype at the retinal periphery ranged from short cilia with severely disrupted discs to reasonably well-organized but abnormally short OS. This phenotype suggests that Kif17 deficiency results in formation of OS that fail to properly elongate. This would be consistent with a role for Kif17 in distal singlet elongation as seen in amphid channel cilia in *C. elegans* (Evans et al., 2006; Peden and Barr, 2005; Snow et al., 2004). Nonetheless, we were surprised by the near complete failure of OS formation in cells with the most complete reduction

NIH-PA Author Manuscript

NIH-PA Author Manuscript

NIH-PA Author Manuscript

in Kif17 protein in the central retina. Elongation of the axoneme was stopped at the level of the basal body in these cells. This is similar to AWB cilia in *C. elegans* in which Kif17 functions independently of the Kif3 complex (Mukhopadhyay et al., 2007).

One possible explanation for the strong phenotype observed in the central retina is that Kif17 performs an essential function in OS assembly distinct from elongation of distal singlets. This hypothetical function comes into play when knockdown at the protein level is complete. For example, disruption of Kif17 function in kidney epithelial cell cultures suggests it plays a role in ciliary membrane protein trafficking that is distinct from cilium elongation (Jenkins et al., 2006). Kif17 may be required for accumulation of visual pigment protein or another critical component in the OS, and failure of this transport could result in failed OS formation in the absence of Kif17.

The unexpectedly strong effect of Kif17 knockdown on OS formation does not preclude a role for Kif17 in distal OS elongation. In fact, these two events could be related. Visual pigments are present in the OS at an extraordinarily high level in excess of 25,000 per μm^2 (Calvert et al., 2001), and are themselves required for assembly of the OS. Rhodopsin mis-localization in both $Tg737^{orpk}$ (Pazour et al., 2002) and Kif3A (Jimeno et al., 2006; Marszalek et al., 2000) deficient photoreceptors has implicated rhodopsin as IFT cargo. Furthermore, homozygous rhodopsin knockout mice form polarized inner segments, but disc formation and outer segment elongation fail completely (Humphries et al., 1997; Lem et al., 1999). This indicates that there is a reciprocal relationship between the assembly of rhodopsin containing membrane and elongation of the OS including its axoneme. Future studies using a conditional knockdown strategy should provide insight into the role of Kif17 in these related events that are essential for OS formation.

Online supplemental material

Refer to Web version on PubMed Central for supplementary material.

Acknowledgements

We thank Dr. Brian Link and Pat Cliff for their help and access to the Medical College of Wisconsin zebrafish facility, and Clive Wells for assistance with EM imaging. This work was supported by NIH grant EY03222 (JCB), a NIH core grant for Vision Research, Medical College of Wisconsin Development Funds (JCB), and NIH grant DK53093 (IAD). C. Insinna was supported by NIH NRSA Training grant T32-EY014537; N. Pathak was supported by NRSA training grant T32-DK007540.

References

Baker SA, Freeman K, Luby-Phelps K, Pazour GJ, Besharse JC. IFT20 links kinesin II with a mammalian intraflagellar transport complex that is conserved in motile flagella and sensory cilia. J Biol Chem 2003;278:34211–8. [PubMed: 12821668]

Calvert PD, Govardovskii VI, Krasnoperova N, Anderson RE, Lem J, Makino CL. Membrane protein diffusion sets the speed of rod phototransduction. Nature 2001;411:90–4. [PubMed: 11333983]

Caspary T, Larkins CE, Anderson KV. The graded response to Sonic Hedgehog depends on cilia architecture. Dev Cell 2007;12:767–78. [PubMed: 17488627]

Corbit KC, Aanstad P, Singla V, Norman AR, Stainier DY, Reiter JF. Vertebrate Smoothened functions at the primary cilium. Nature 2005;437:1018–21. [PubMed: 16136078]

Eggenschwiler JT, Anderson KV. Cilia and developmental signaling. Annu Rev Cell Dev Biol 2007;23:345–73. [PubMed: 17506691]

Evans JE, Snow JJ, Gunnarson AL, Ou G, Stahlberg H, McDonald KL, Scholey JM. Functional modulation of IFT kinesins extends the sensory repertoire of ciliated neurons in Caenorhabditis elegans. J Cell Biol 2006;172:663–9. [PubMed: 16492809]

NIH-PA Author Manuscript

NIH-PA Author Manuscript

NIH-PA Author Manuscript

Guillaud L, Setou M, Hirokawa N. KIF17 dynamics and regulation of NR2B trafficking in hippocampal neurons. J Neurosci 2003;23:131–40. [PubMed: 12514209]

Hou Y, Qin H, Follit JA, Pazour GJ, Rosenbaum JL, Witman GB. Functional analysis of an individual IFT protein: IFT46 is required for transport of outer dynein arms into flagella. J Cell Biol 2007;176:653–65. [PubMed: 17312020]Epub 2007 Feb 20

Humphries MM, Rancourt D, Farrar GJ, Kenna P, Hazel M, Bush RA, Sieving PA, Sheils DM, McNally N, Creighton P, Erven A, Boros A, Gulya K, Capecchi MR, Humphries P. Retinopathy induced in mice by targeted disruption of the rhodopsin gene. Nat Genet 1997;15:216–9. [PubMed: 9020854]

Jenkins PM, Hurd TW, Zhang L, McEwen DP, Brown RL, Margolis B, Verhey KJ, Martens JR. Ciliary targeting of olfactory CNG channels requires the CNGB1b subunit and the kinesin-2 motor protein, KIF17. Curr Biol 2006;16:1211–6. [PubMed: 16782012]

Jimeno D, Feiner L, Lillo C, Teofilo K, Goldstein LS, Pierce EA, Williams DS. Analysis of kinesin-2 function in photoreceptor cells using synchronous Cre-loxP knockout of Kif3a with RHO-Cre. Invest Ophthalmol Vis Sci 2006;47:5039–46. [PubMed: 17065525]

Kayadjanian N, Lee HS, Pina-Crespo J, Heinemann SF. Localization of glutamate receptors to distal dendrites depends on subunit composition and the kinesin motor protein KIF17. Mol Cell Neurosci 2007;34:219–30. [PubMed: 17174564]

Lem J, Krasnoperova NV, Calvert PD, Kosaras B, Cameron DA, Nicolo M, Makino CL, Sidman RL. Morphological, physiological, and biochemical changes in rhodopsin knockout mice. Proc Natl Acad Sci U S A 1999;96:736–41. [PubMed: 9892703]

Lin F, Hiesberger T, Cordes K, Sinclair AM, Goldstein LS, Somlo S, Igarashi P. Kidney-specific inactivation of the KIF3A subunit of kinesin-II inhibits renal ciliogenesis and produces polycystic kidney disease. Proc Natl Acad Sci U S A 2003;100:5286–91. [PubMed: 12672950]

Marszalek JR, Liu X, Roberts EA, Chui D, Marth JD, Williams DS, Goldstein LS. Genetic evidence for selective transport of opsin and arrestin by kinesin-II in mammalian photoreceptors. Cell 2000;102:175–87. [PubMed: 10943838]

Mukhopadhyay S, Lu Y, Qin H, Lanjuin A, Shaham S, Sengupta P. Distinct IFT mechanisms contribute to the generation of ciliary structural diversity in C. elegans. Embo J 2007;26:2966–80. [PubMed: 17510633]

Pan J, Wang Q, Snell WJ. Cilium-generated signaling and cilia-related disorders. Lab Invest 2005;85:452–63. [PubMed: 15723088]

Pan X, Ou G, Civelekoglu-Scholey G, Blacque OE, Endres NF, Tao L, Mogilner A, Leroux MR, Vale RD, Scholey JM. Mechanism of transport of IFT particles in C. elegans cilia by the concerted action of kinesin-II and OSM-3 motors. J Cell Biol 2006;174:1035–45. [PubMed: 17000880]

Pazour GJ, Baker SA, Deane JA, Cole DG, Dickert BL, Rosenbaum JL, Witman GB, Besharse JC. The intraflagellar transport protein, IFT88, is essential for vertebrate photoreceptor assembly and maintenance. J Cell Biol 2002;157:103–13. [PubMed: 11916979]

Peden EM, Barr MM. The KLP-6 kinesin is required for male mating behaviors and polycystin localization in Caenorhabditis elegans. Curr Biol 2005;15:394–404. [PubMed: 15753033]

Qin H, Burnette DT, Bae YK, Forscher P, Barr MM, Rosenbaum JL. Intraflagellar transport is required for the vectorial movement of TRPV channels in the ciliary membrane. Curr Biol 2005;15:1695–9. [PubMed: 16169494]

Rohatgi R, Milenkovic L, Scott MP. Patched1 regulates hedgehog signaling at the primary cilium. Science 2007;317:372–6. [PubMed: 17641202]

Roof D, Adamian M, Jacobs D, Hayes A. Cytoskeletal specializations at the rod photoreceptor distal tip. Journal of Comparative Neurology 1991;305:289–303. [PubMed: 1902849]

Rosenbaum JL, Witman GB. Intraflagellar transport. Nat Rev Mol Cell Biol 2002;3:813–25. [PubMed: 12415299]

Schneider L, Clement CA, Teilmann SC, Pazour GJ, Hoffmann EK, Satir P, Christensen ST. PDGFRalphaalpha signaling is regulated through the primary cilium in fibroblasts. Curr Biol 2005;15:1861–6. [PubMed: 16243034]

Setou M, Nakagawa T, Seog DH, Hirokawa N. Kinesin superfamily motor protein KIF17 and mLin-10 in NMDA receptor-containing vesicle transport. Science 2000;288:1796–802. [PubMed: 10846156]

NIH-PA Author Manuscript

NIH-PA Author Manuscript

NIH-PA Author Manuscript

Snow JJ, Ou G, Gunnarson AL, Walker MR, Zhou HM, Brust-Mascher I, Scholey JM. Two anterograde intraflagellar transport motors cooperate to build sensory cilia on C. elegans neurons. Nat Cell Biol 2004;6:1109–13. [PubMed: 15489852]

Steinberg RH, Wood I. Clefts and microtubules of photoreceptor outer segments in the retina of the domestic cat. J Ultrastruct Res 1975;51:307–403. [PubMed: 1138108]

Thisse C, Thisse B, Schilling TF, Postlethwait JH. Structure of the zebrafish snail1 gene and its expression in wild-type, spadetail and no tail mutant embryos. Development 1993;119:1203–15. [PubMed: 8306883]

Vihtelic TS, Doro CJ, Hyde DR. Cloning and characterization of six zebrafish photoreceptor opsin cDNAs and immunolocalization of their corresponding proteins. Visual Neurosci 1999;16:571–585.

Webber WA, Lee J. Fine structure of mammalian renal cilia. Anat Rec 1975;182:339–43. [PubMed: 1155803]

NIH-PA Author Manuscript
NIH-PA Author Manuscript
NIH-PA Author Manuscript

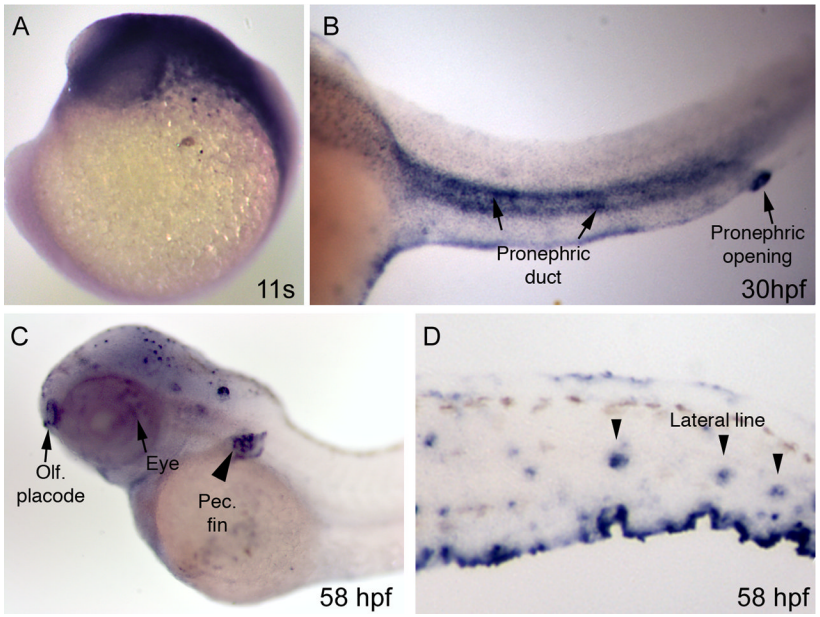

Figure 1. Analysis of Kif17 expression in whole embryos by in situ hybridization

A. At the 11 somite stage, kif17 is expressed broadly in the head region. **B.** At 30 hpf, Kif17 is observed in the pronephros and strongly in the pronephric opening (arrow). **C.** At 58 hpf, expression is observed in the eye (arrow), olfactory placode (arrow), the forming pectoral fin (arrowhead), and **(D)** in the lateral line organs.

NIH-PA Author Manuscript
NIH-PA Author Manuscript
NIH-PA Author Manuscript

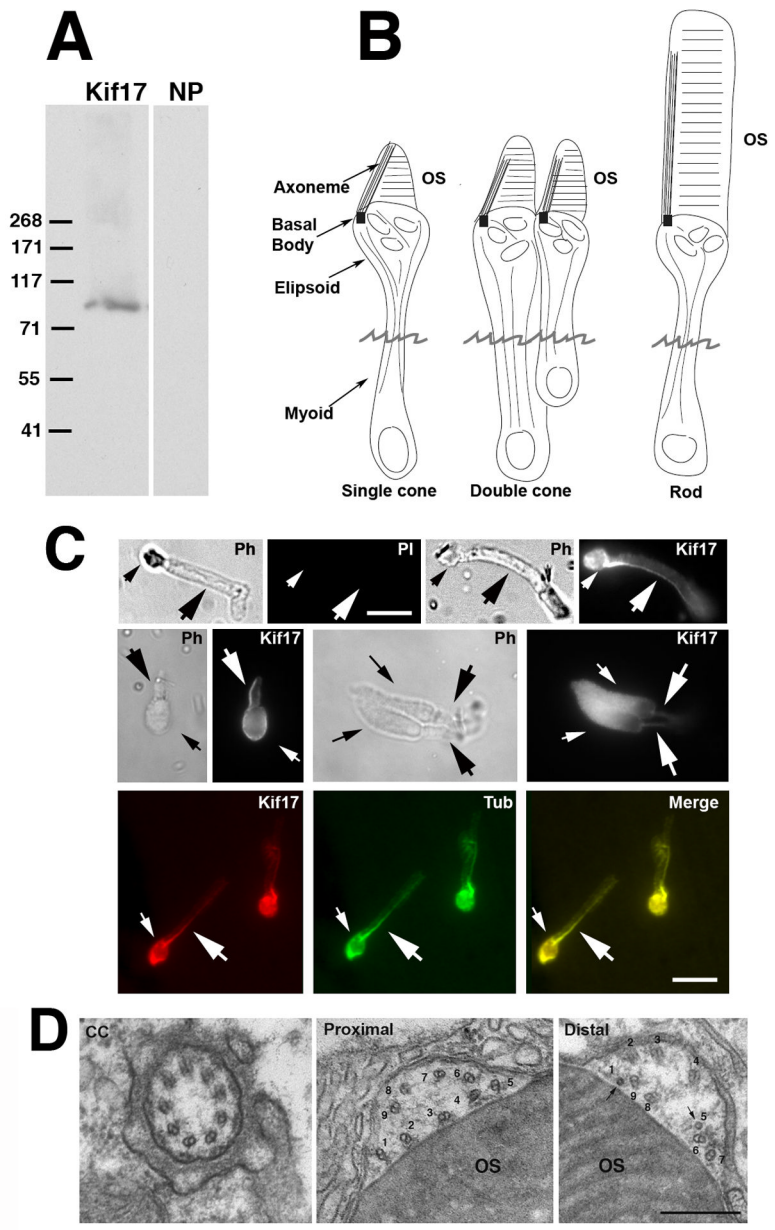

Figure 2. Immunocytochemical (IC) localization of Kif17 in photoreceptors

A. Immunoblot of 3 day zebrafish embryo lysate. The Kif17 band corresponds to the predicted size based on the zebrafish cDNA sequence; NP, no primary antibody. **B.** Three morphological types of zebrafish photoreceptors; isolated photoreceptors break off at the position of the jagged line. **C.** IC of Kif17 in isolated adult zebrafish photoreceptors. Ph, Upper left is a phase (PH), and no primary antibody control image (PI) of a rod. Upper right is a phase and a Kif17 stained rod. Middle panel is a phase and Kif17 stained single cone (left), and double cone (right). Lower panel shows co-localization of Kif17 (left) with acetylated α-tubulin (middle) along the axoneme of a rod. Small arrows point to the ellipsoid region and the large arrows point to axoneme in the OS. Bar = 10 μm. **D.** EM images at the level of the connecting cilium (CC), the proximal OS, and more distal OS of a developing cone from a 3 day zebrafish larva. Note that both the proximal and distal OS images are within the most proximal one third of the OS.

Doublets adjacent to the discs are numbered 1–9; the more distal image shows two singlets (1 and 5) and 7 doublets adjacent to the OS discs. Bar= 0.33 μm.

NIH-PA Author Manuscript
NIH-PA Author Manuscript
NIH-PA Author Manuscript

NIH-PA Author Manuscript
NIH-PA Author Manuscript
NIH-PA Author Manuscript

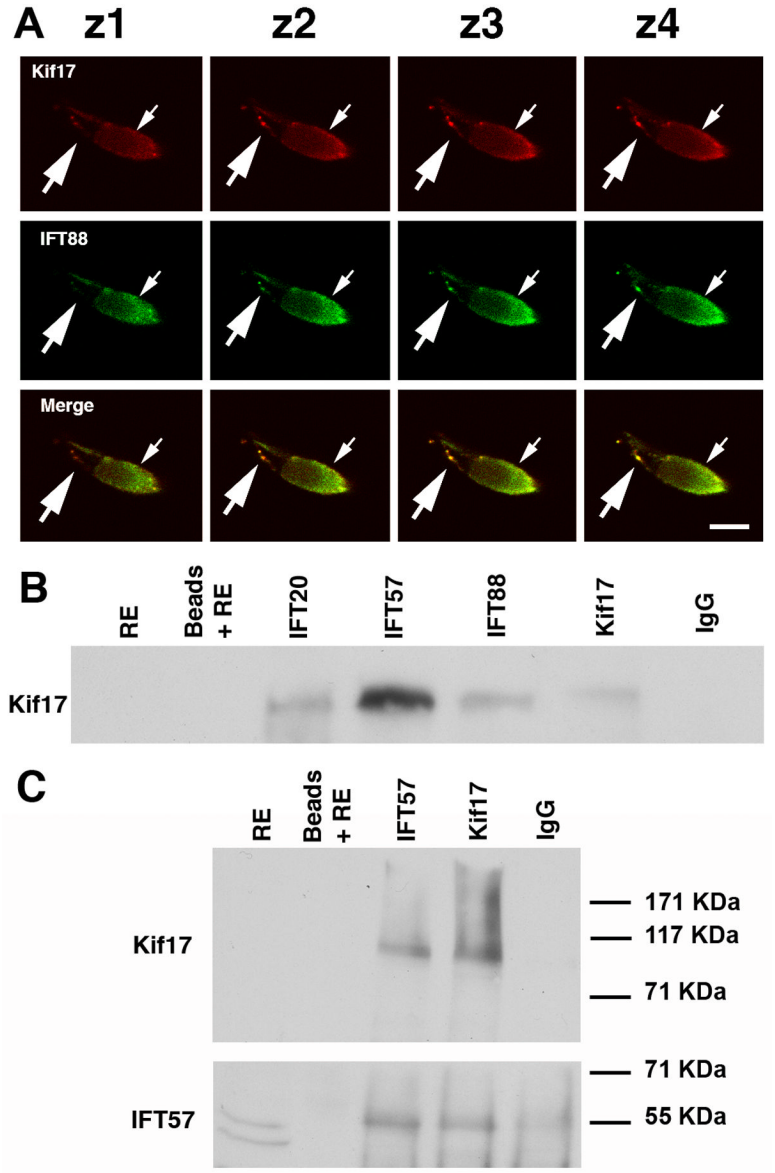

Figure 3. Association of Kif17 with IFT complex proteins

A. Consecutive confocal Z-slices of a cone double labeled with Kif17 and IFT88 antibodies. The small arrow indicates the position of the ellipsoid and the large arrow points to punctate staining along the axoneme. Bar = 10 μm. **B**. Co-immunoprecipitation of Kif17 with antibodies to IFT20, IFT57, IFT88, and Kif17. IP antibodies are shown at the top and western blot antibodies on the left. Kif17 was not detected in the RE, which was at 1/5 of the volume used for IP; Kif17 was readily detected when the extract load was higher (see Fig. 1A). Beads plus RE without antibody and a mixture of IgG1 and IgG2 were used as controls for non-specific binding. In separate gels, IFT antibodies were shown to co-IP using anti-IFT antibodies in zebrafish as previously shown for mouse retina (Baker, et al., 2003). **C.** IP experiment as in B in which the blot was cut into two pieces; the upper portion was stained for Kif17 and lower portion for IFT57. Note that as reported in mice (Pazour, et al., 2002), two bands are detected with the IFT57 antibody but only the upper band is present in the co-IPs.

NIH-PA Author Manuscript
NIH-PA Author Manuscript
NIH-PA Author Manuscript

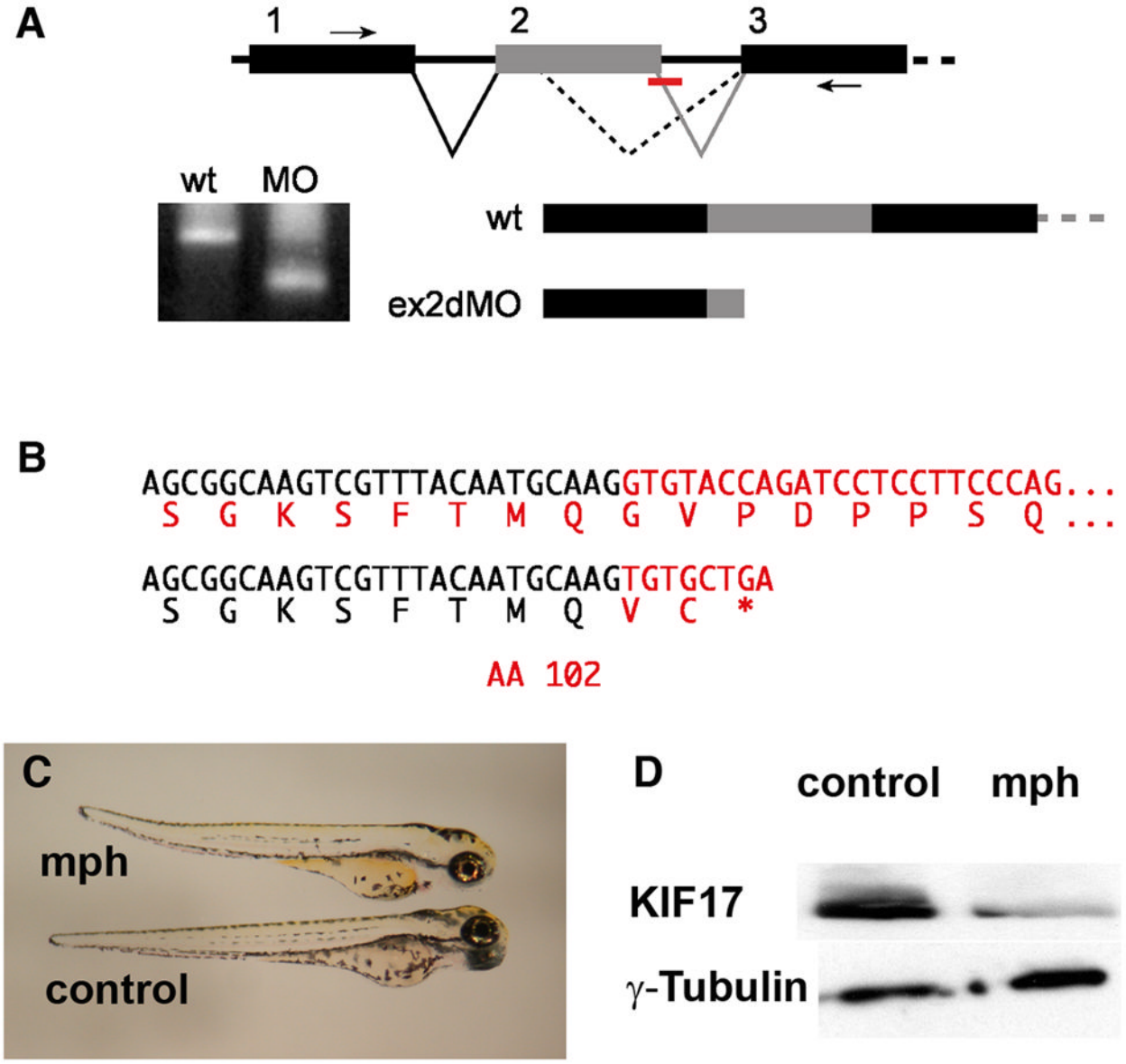

Figure 4. Disruption of *Kif17* splicing by an antisense morpholino oligonucleotide

A. Mis-splicing of the *Kif17* mRNA caused by blocking the exon 2 donor sequence. RT-PCR primers in exons 1 and 3 (small arrows) generate a smaller product in morphant embryos. **B.** The morphant RT-PCR product sequence reveals an out of frame fusion to a cryptic splice donor within exon 2 resulting in a mRNA predicted to encode a Kif17 protein truncated at amino acid 102. **C.** Morphant (mph) and control (invert sense) injected 3 day zebrafish larvae. **D.** Western blots of 3 day embryos showing the reduction of Kif17 in morphants; anti-γ-tubulin was used as a loading control.

NIH-PA Author Manuscript
NIH-PA Author Manuscript
NIH-PA Author Manuscript

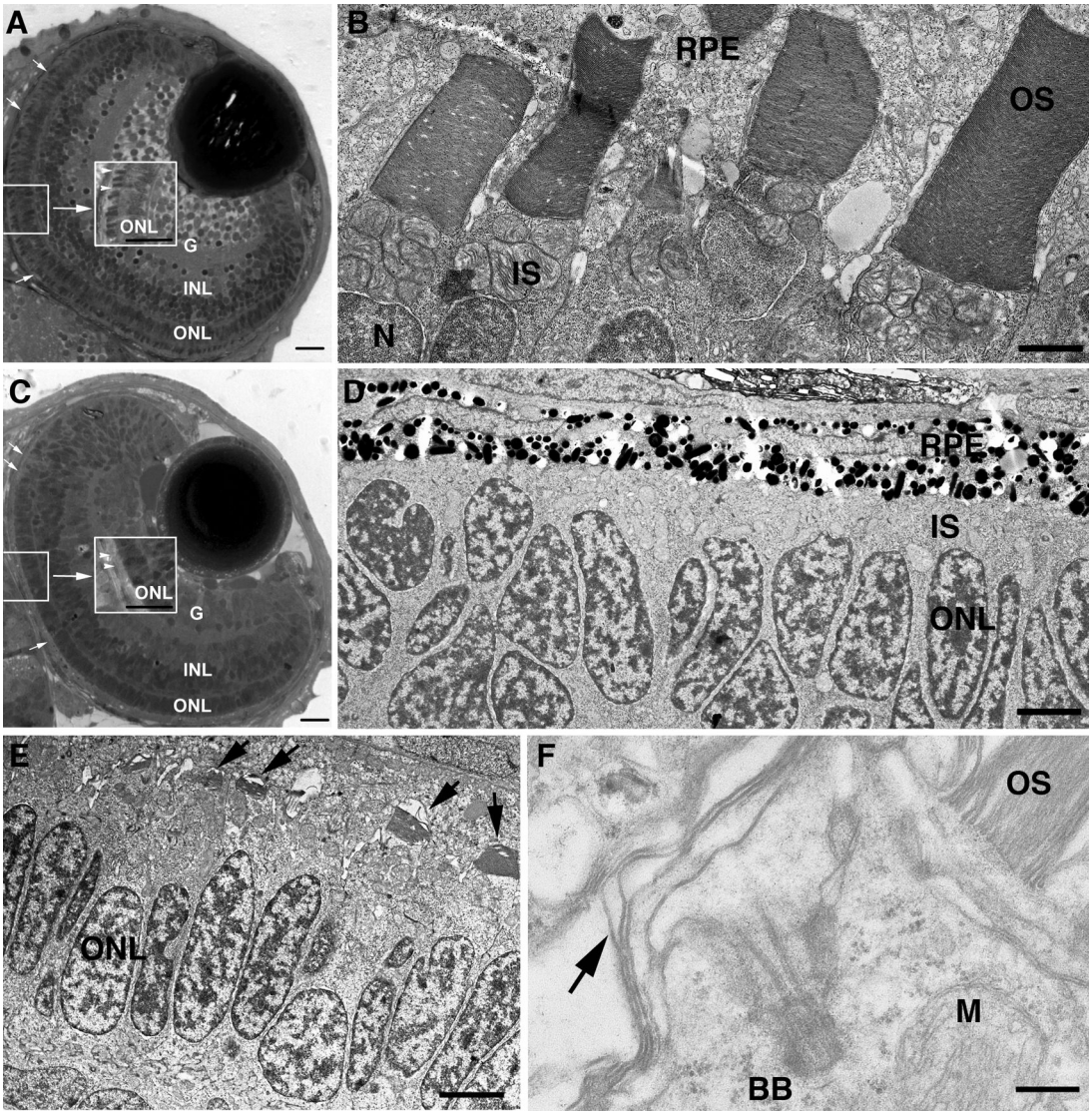

Figure 5. Disrupted photoreceptor OS formation in *Kif17* morphants

A. WT eye of a 3 day old embryo. The lens and retinal lamination are well developed. OSs (small arrows, center inset) have developed throughout the retina. G, ganglion cell layer; INL, inner nuclear layer; ONL, outer nuclear layer (photoreceptor nuclei). Bar = 10 μm. **B.** EM view of junction between photoreceptors and retinal pigment epithelium (RPE) in WT showing mitochondria rich inner segments (IS) and the lamellar OSs; N, photoreceptor nucleus. Bar = 2.5 μm. **C.** Morphant eye of a 3 day old embryo shows normal retinal lamination but lack of OS (small arrow, center inset). Bar = 10 μm. **D.** EM view of junction between photoreceptors and RPE in a morphant; IS layer is visible between nuclei (ONL) and RPE, but OS are not present. Bar = 5 μm. **E.** EM view of junction between photoreceptors and RPE of a morphant with short, under-developed OS (arrows). Bar = 6.6 μm. **F.** High power EM view of a photoreceptor showing the basal body (BB) at the base of the cilium; arrow indicates disorganized OS discs. M, mitochondrion. OS (upper right) is from an adjacent photoreceptor. Bar = 0.5 μm.

NIH-PA Author Manuscript

NIH-PA Author Manuscript

NIH-PA Author Manuscript

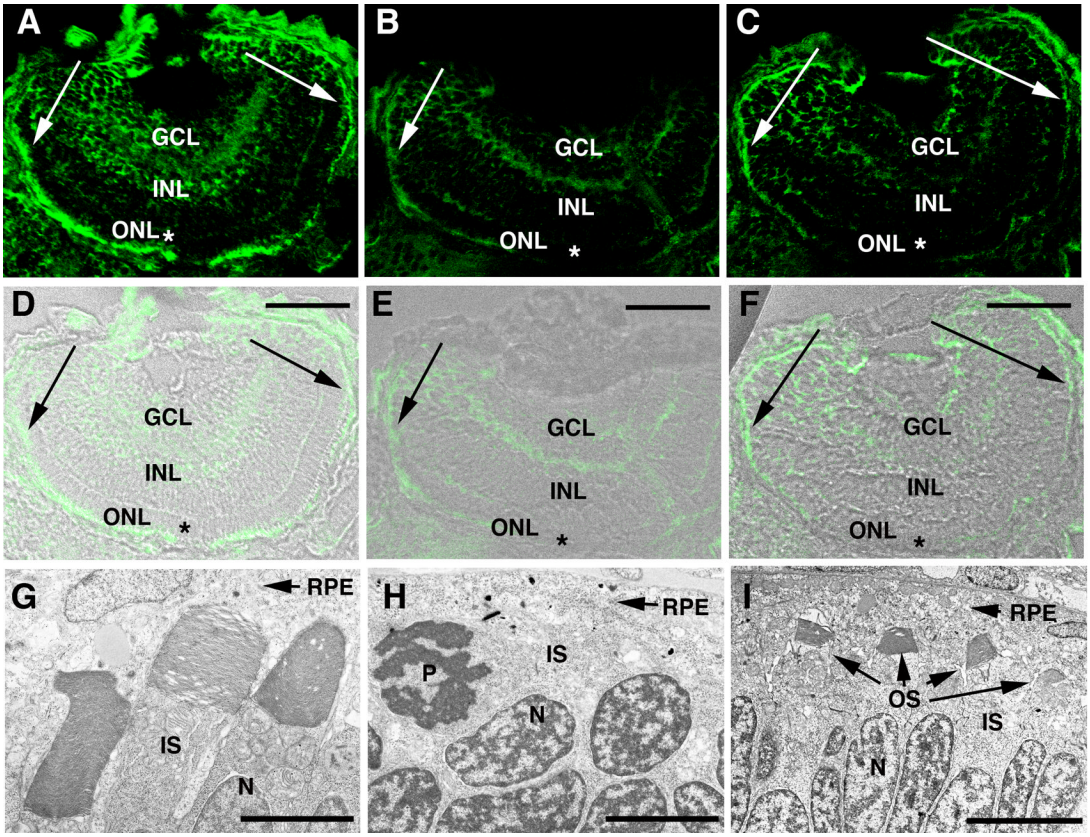

Figure 6. Correlation between photoreceptor OS loss and extent of Kif17 knockdown in morphants

A–C Kif17 distribution in eyes of 3 day old control (A) and morphant larvae (B,C). **D–F.** IC images A–C merged with bright-field images of the same sections. Abbreviations: GCL, ganglion cell layer; INL, inner nuclear layer; and ONL, outer nuclear layer. Scale bars in D–F = 40 μm. Note that in the photoreceptor layer of the early developing central retina (asterisks) of morphants Kif17 immunoreactivity is almost completely lacking but in the late developing periphery (indicated by arrows), Kif17 protein is present. **G–I.** EM images from the central region of a control retina (G), and of a morphant retina (**H**). I is from the peripheral region of a morphant retina. Note that OS form throughout the retina of controls and are virtually absent from the central retina of morphants where Kif17 protein knock-down is most complete. OS are seen in the periphery of some but not all morphants. EM magnifications bars: 2.8 μm (**G**), 4.0 μm (**H**), and 6.8 μm (**I**).

NIH-PA Author Manuscript

NIH-PA Author Manuscript

NIH-PA Author Manuscript

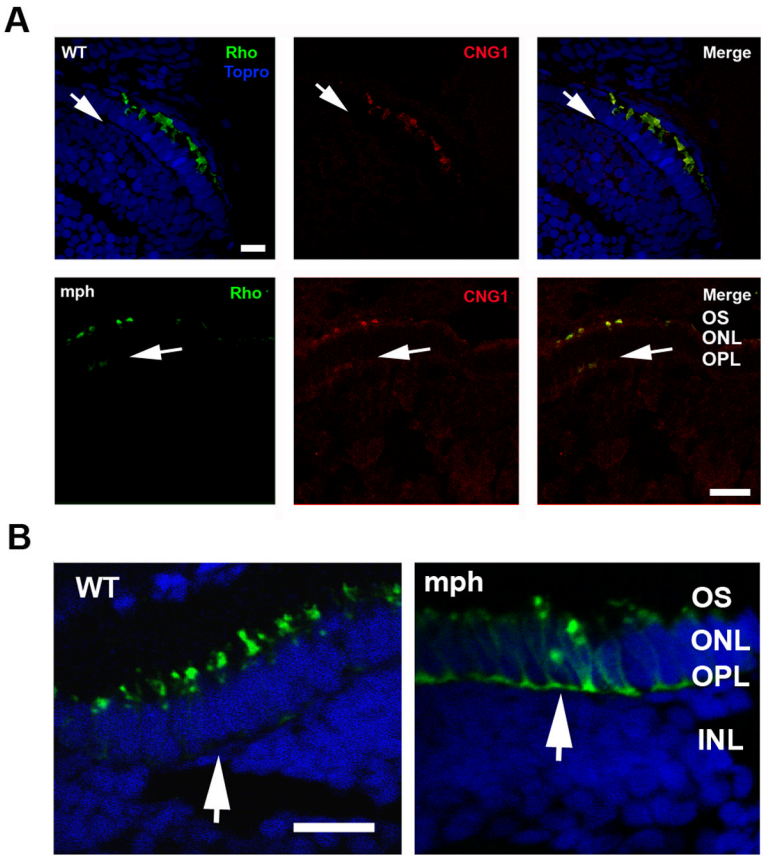

Figure 7. Mis-localization of the photopigment apoprotein in cones and to a lesser extent in rods of morphants

A. (Upper panel) Double label of rhodopsin (green) and CNG1 (red) in rods of 3 day old control (WT) and morphants. Topro (blue) was used in the control (WT) to show the nuclear layers. Note that Rho and CNG1 co-localize in the OS in control (WT) and are undetectible in the outer plexiform layer (arrows). (Lower panel) In contrast to control (WT), both Rho and CNG1 are seen in the outer plexiform (synaptic) layer of morphants (arrows). Bar = 20.55μm. **B.** Cone opsin (green) is very extensively mis-localized to the perinuclear region and outer plexiform layer (synaptic layer) in morphant (mph) cones compared to control (see arrows). Sections are double labeled with Topro (blue) to show the nuclear layers. Bar = 12.5 μm.

NIH-PA Author Manuscript

NIH-PA Author Manuscript

NIH-PA Author Manuscript

Table 1

Cilia Length Measurement in Pronephric duct.

	Anterior	**Middle**	**Distal**
Kf17Con	12.2 +/− 2.2 μm n=21	10.9 +/− 1.9 μm n=12	7.5 +/− 1.3 μm n=10
Kf17X2dMo	12.4 +/− 2.24 μm n=36	11.7 +/− 1.9 μm n=22	6.6 +/−1.65 μm n=16
Pronephric Cilia Beat Frequency			
		Beat Frequency	
Kf17CoMo		29 Hz	
Kf17X2dMo		29 Hz	